In situ Visualization of Lithium Ion Intercalation into MoS_2 Single Crystals using Differential Optical Microscopy with Atomic Layer Resolution

Mukkannan Azhagurajan,[†] Tetsuya Kajita,[‡] Takashi Itoh,[‡] Youn-Geun Kim,[§] and Kingo Itaya*[,†,‡]

[†]Institute of Multidisciplinary research for Advanced Materials, Tohoku University, 2-1-1 Katahira, Sendai 980-8577, Japan

[‡]Frontier Research Institute for Interdisciplinary Sciences, Tohoku University, 6-3 Aoba, Sendai 980-8578, Japan

[§] Division of Chemistry and Chemical Engineering, Joint Center for Artificial Photosynthesis , California Institute of Technology, Pasadena, California 91125, United States

Correspondence to: itaya@atom.che.tohoku.ac.jp

Supporting Information

Materials and Methods

LCM-DIM is a new advanced optical technique developed for the *in situ* detection of surface steps as reported by Sazaki. [1-3] Our system employs a confocal system (FV300, Olympus) attached to an inverted optical microscope (IX70, Olympus) equipped with a Nomarski prism introduced into the optical path and a partially coherent superluminescent diode (Amonics Ltd., Model ASLD68-050-B-FA:680 nm) to eliminate interference patterns. To achieve single atomic step resolution, conventional polymer-based polarizers and analyzers were replaced by ones made of Ag nanoparticles (CODIXX AG Germany: color Pol VISIRCWO2); consequently, the light intensity at the position of the photomultiplier was increased by one order of magnitude.[4] Two objective lenses (LUCPLFLN 20 and LUCPLEFLN 40 Olympus) were used to resolve single atomic steps on metals and semiconductors. The diameter of the confocal aperture was 100 μm.

The electrochemical cell was connected to a high-vacuum system as shown in Fig. 1S. Vacuum-tight electrochemical cells with three electrode configuration were filled with the ionic liquid and heated at 130°C using an oil bath for more than 10 hours until the vacuum level was less than 1×10^{-5} Pascal to remove water.

It is important to note that the optical system was constructed for measurements to be done in air. Our system has an additional lens to achieve atomic height resolution in solution. The additional lens can compensate difference in refractive indexes between air and liquids. In order

to achieve atomic height resolution, the total length between the surface of samples and the bottom of the cell must be less than *ca.* 2 mm. Because the thickness of an optically flat Pyrex glass plate is 0.5 mm, the maximum thickness of solution should be less than 1.5 mm. Fig.S2 shows a detailed configuration of the optical system coupled with the electrochemical cell.

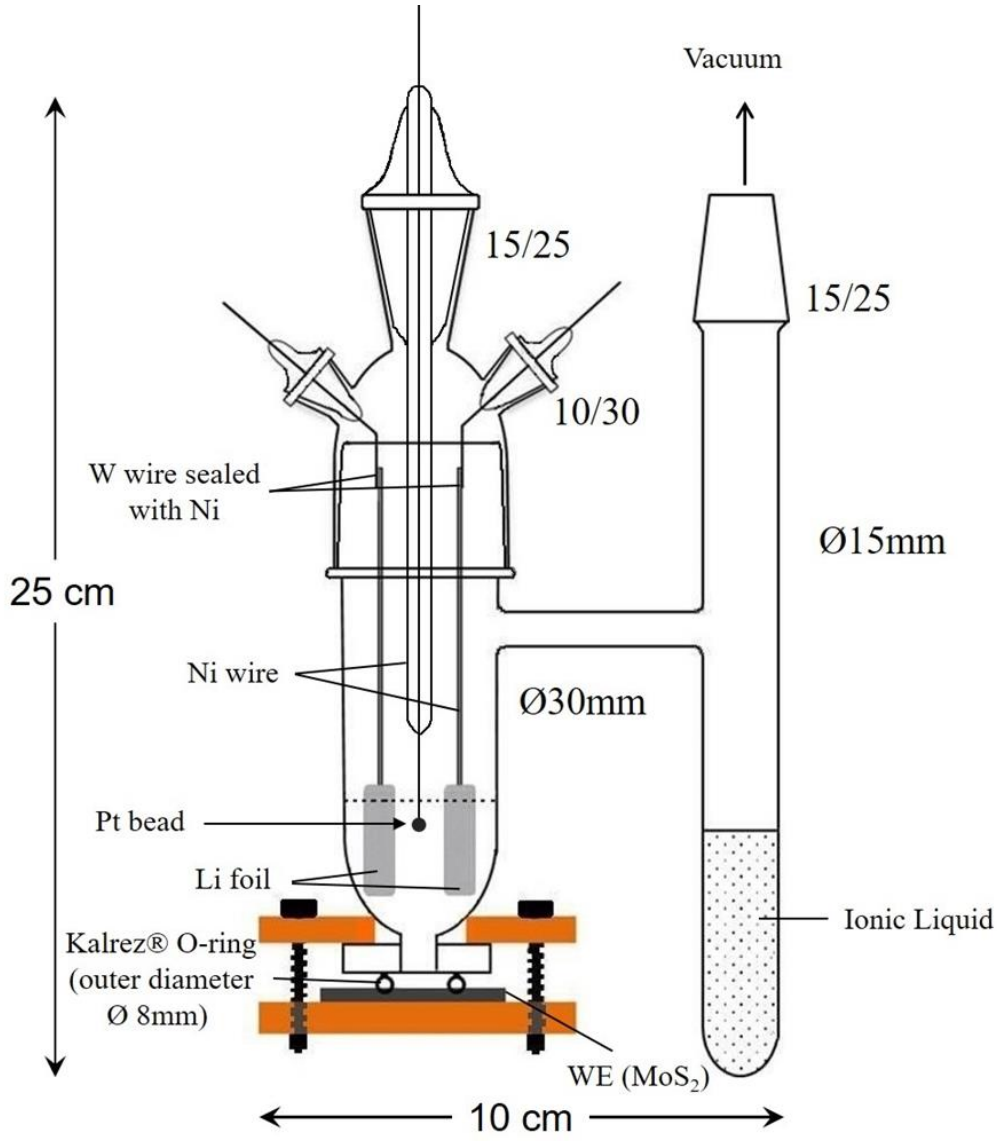

Figure S1. Schematic diagram of the high-vacuum electrochemical cell for cyclic voltammetry. The electrochemical cell has three joints at the top: two angled ports were used for Li reference and Li counter electrodes, and a middle port where a Pt bead was placed to measure the background current of the ionic liquid. The MoS_2 single-crystal working electrode was inserted at the bottom of the cell, such that the basal plane of the crystal was in contact with the electrochemical solution.

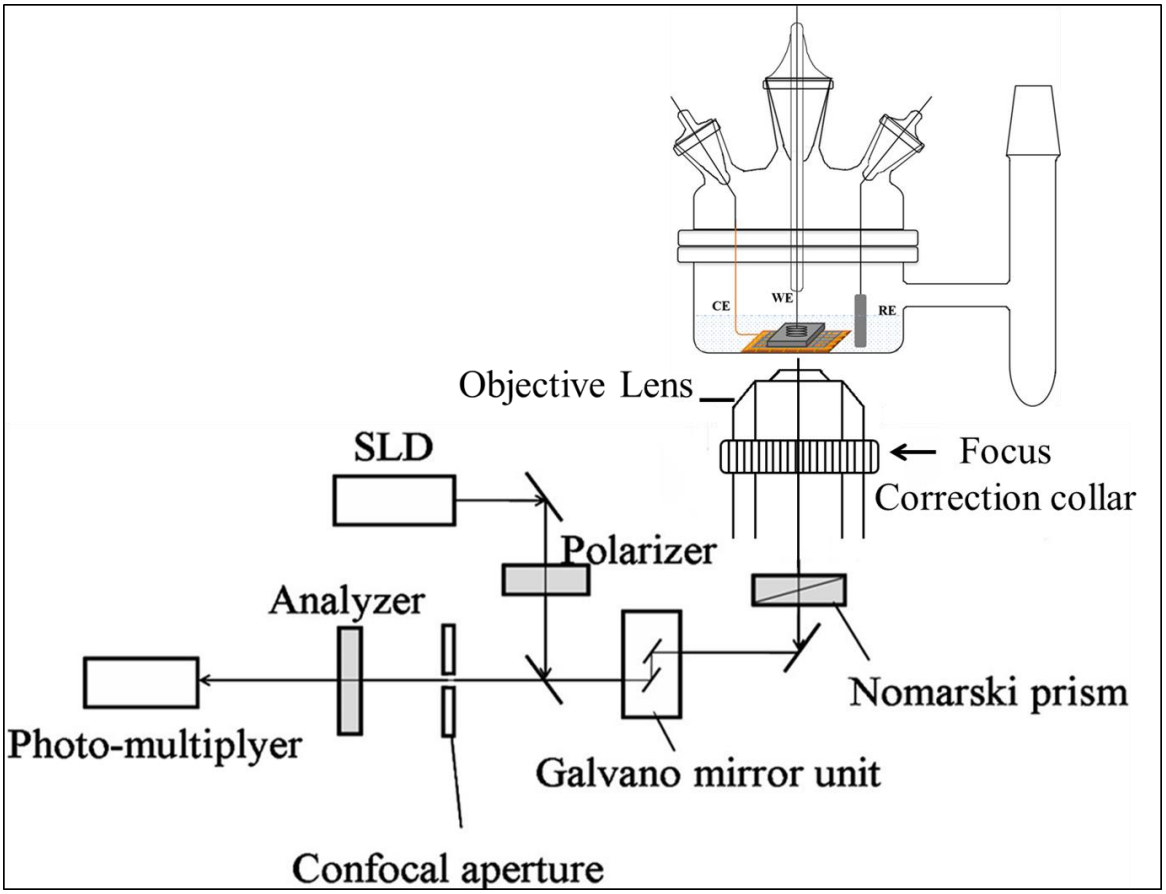

Figure S2 Schematic diagram of LCM-DIM system combined with electrochemical cell. To achieve atomic-height resolution in solution, a specially designed objective lens with a compensator (focus correction collar) was used to adjust the focus point caused by changes in the refraction index by the solution and the glass plate.

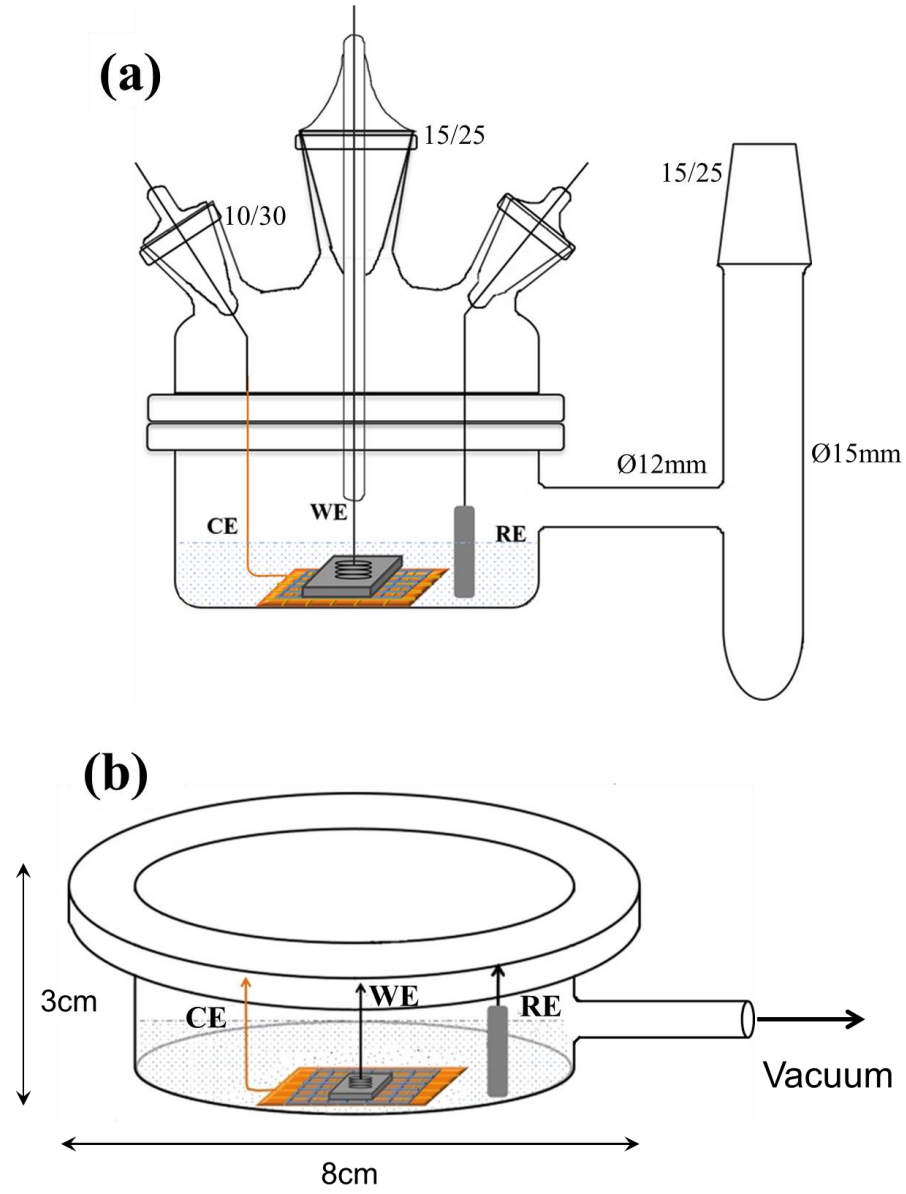

Figure S3. (a) Schematic diagram of LCM-DIM electrochemical cell. (**b**) Enlarged view of the bottom section of the electrochemical cell. The counter electrode (CE) is made of gold mesh (Gilder Au 100) with 20 mm x 20 mm grid size, a thickness of 5μm, and a mesh size of 100 μm. A Teflon mesh is placed between the gold mesh and the working electrode (WE) in order to avoid electric contact. The Teflon mesh has a grid size of 15 mm x 15 mm and a thickness of 0.5 mm; the diameter of the hole is 0.6 mm. The sample electrode (MoS_2) can be viewed through the open windows of the gold and Teflon meshes.

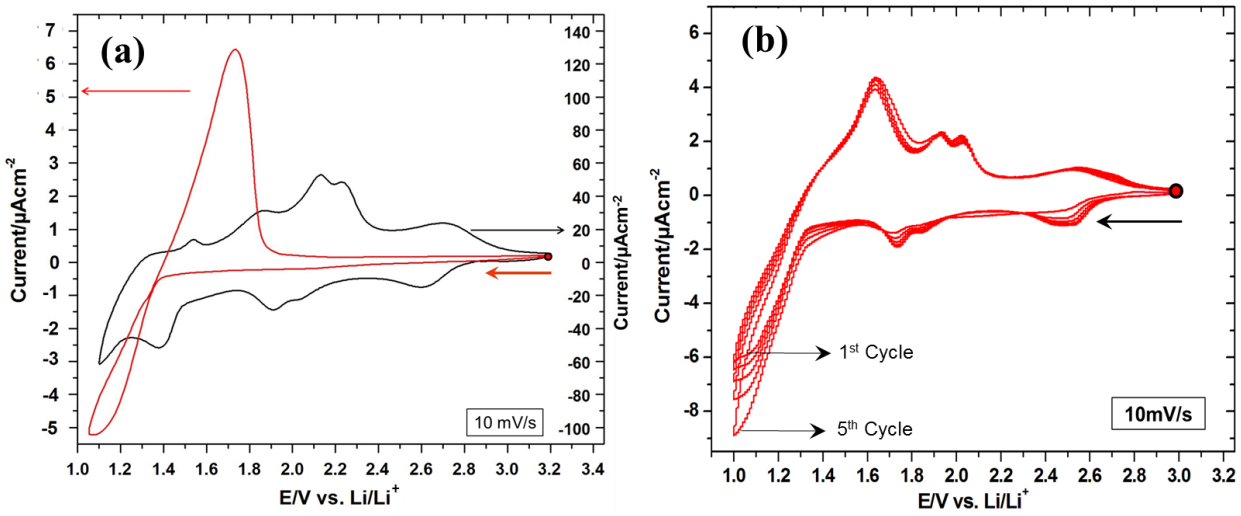

Figure S4. (a) Voltammetric profiles of MoS_2 in an ionic liquid at a scan rate of 10 mV s^{-1} at two different conditions. (Red trace): under high-vacuum pressure of 1 x 10^{-5} Pascal at 130ºC; (Black trace): inside a glove box using as-received solvents. The emergence of multiple voltammetric peaks in the unpurified solvents is ascribed to the reduction of water impurities. The scale for the current densities of the black and red traces differs by two orders of magnitude. The electrolyte solution contains 0.32 mol lithium bis(trifluoromethylsulfonyl)imide (LiTFSI) (Kanto Chem. Co.) per kg of 1-ethyl-3-methylimidazolium bis(fluorosulfonyl)imide (EMI-FSI). (b) Cyclic voltammogram of MoS_2 in a battery-grade organic electrolyte of 1:1 (by volume) ethylene carbonate and diethyl carbonate (Kanato Chem. Co.) in 1 *M* $LiClO_4$ solution at a scan rate of 10 mVs^{-1}.

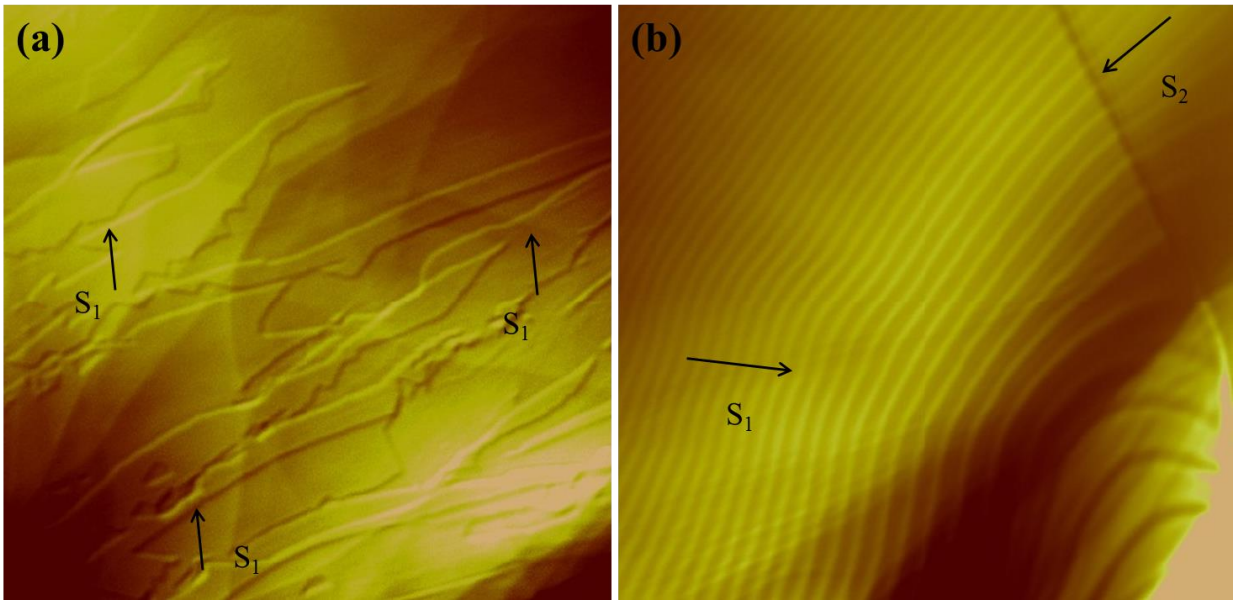

Figure S5. Ultra-flat surfaces with the single atomic step of carefully cleaved MoS_2 single crystals. (a) The arrows labeled S_1 corresponds to the monoatomic step. (b) An unusually flat surface with long-range array of the monoatomic step (S_1) with only one diatomic step (S_2). Both image sizes were 140 x 140 μm. The height of steps and the width of terraces are strongly depend on cleaving techniques. Usually, multi-atomic steps were usually appeared as described in the text.

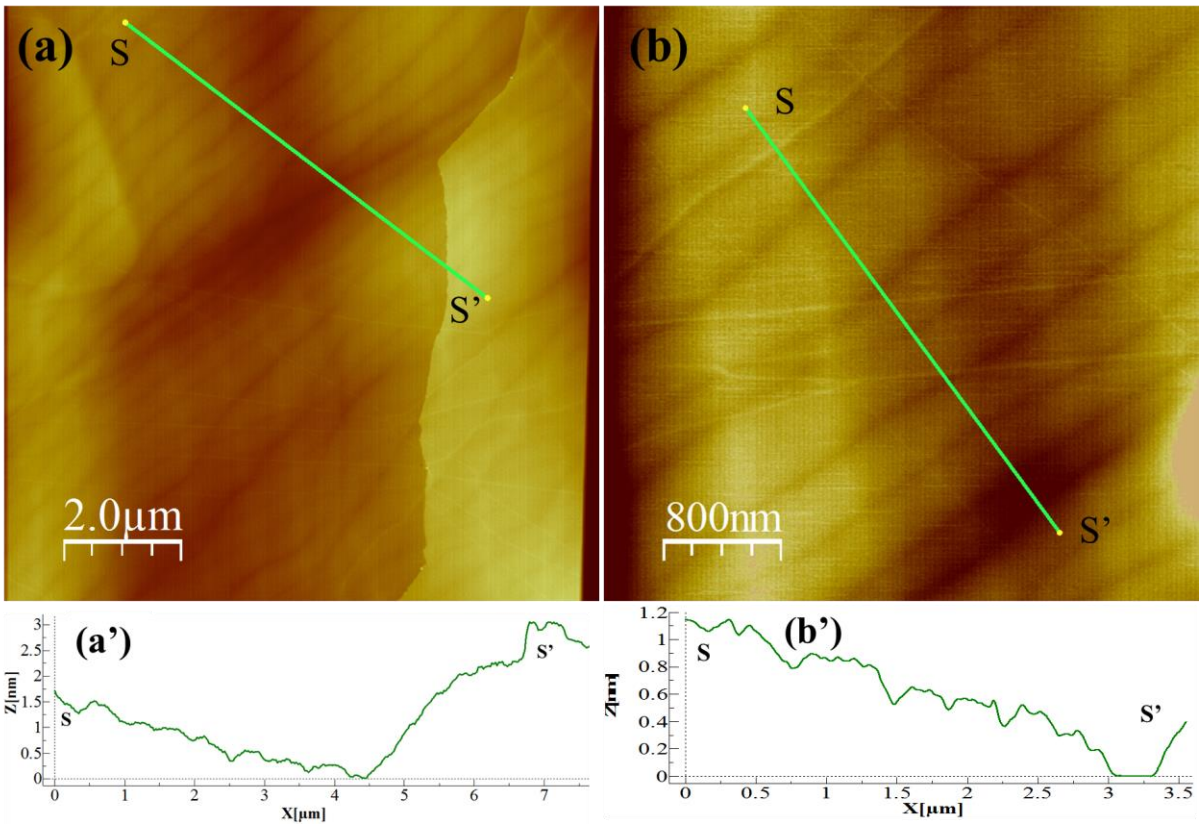

Figure S6. High-resolution EC-STM images obtained in air. Stacking of MoS_2 terraces leads to the formation of steps with less than a monoatomic (sub-monoatomic) step height. (a) A wide-scan view of the MoS_2 surface showing line profile (S-S') that compares monoatomic and sub-monoatomic step heights. The height of the monoatomic steps in (a') is 3 to 4 times larger than that of the sub-monoatomic steps. (b) A high-resolution view shows a series of terraces that expose sub-monoatomic steps. The line profile (S-S') in (b') indicates a near-uniform height of 0.1-0.2 nm for all the sub-monoatomic steps which resembles the quantitative examination of bending of graphene layer across Ir step edges observed by J. Coraux et.al.[5] The images of (a) and (b) were taken in an area of 10 x 10 µm and 4 x 4 µm, respectively.

Caption for Movie S1. Real-time *in situ* LCM-DIM video capture of Li-ion intercalation into the first layer beneath the selvedge of a MoS_2 single crystal in an electrolyte solution of lithium bis(trifluoromethylsulfonyl)imide (LiTFSI) and 1-ethyl-3-methylimidazolium bis(fluorosulfonyl)imide (EMI-FSI). The movie corresponds to the dynamic process depicted in Figure 2 (a-c). The movie shows the electrode events at a potential 5 mV more negative than the open-circuit potential (OCP). The movie corresponds to the process in Figure 2 (d-f). It is interesting that the de-intercalation reactions occurred in a reversed way. Li ions in the lower layers were de-intercalated, disappearing the domains as shown in movie and the de-intercalation reactions were also occurred by a layer-by-layer mode as can be seen in movie.

Caption for Movie S2. Real-time *in situ* LCM-DIM video capture of extensive Li-ion intercalation involving multilayers of the MoS_2 in LiTFSI and EMI-FSI electrolyte solution at -1.2 V vs Li/Li^+. Intercalation of the second (l_2), third (l_3), and fourth (l_4) layers registers as domains with different contrast. The movie shows that the de-intercalation follows the reversed pathway of intercalation; i.e. Li ions in the subsurface layers are initially de-intercalated. The disappearance of the lithiated domains occurs layer-by-layer mode, leaving behind an atomically flat surface. When the potential was shifted positively by only a few mV, de-intercalation proceeded similarly as that shown in **Movie S1**.

Caption for Movie S3. Real-time *in situ* LCM-DIM video capture of Li-ion intercalation and de-intercalation involving several MoS_2 layers. To reveal surface structural changes during extensive intercalation, the electrode potential was further scanned to 1.1 V, where the current for the intercalation was ca. 12 $\mu A/cm^2$. The intercalated layers appeared as dark domains, in a manner similar to what was observed at low intercalation current densities. The bright veins of the reticulation suggested that Li ions existed in multilayers along these lines. After the acquisition of the intercalation reactions, the electrode potential was scanned to 1.4 V at 50 mV s^{-1} to spur de-intercalation. Many of the intercalated domains gradually disappeared with concomitant changes in contrast similar to those of **Movie S2**. However, the reticulation persisted even after 15 min at 1.8 V.

Caption for Movie S4. Real-time *in situ* LCM-DIM video capture of Li-ion intercalation involving several MoS_2 layers at 0.9 V vs Li/Li^+ induced intercalation at a rapid rate. Each image was acquired 0.25 sec/frame. Based on the contrast variation, several layers were simultaneously involved in the intercalation process. Upon further intercalation, the domains expanded into patchy reticulated regions similar to those in Figure 8. However, the intercalated domains appeared smaller, implying that fast intercalation led to a decrease in domain size. At this negative potential, the step edges exhibit many defect sites at which intercalation is initiated. Under this condition, several layers are simultaneously involved in the intercalation.

Caption for Move S5. Real-time *in situ* LCM-DIM video capture of Li-ion intercalation at the different area of the same sample under the identical experimental condition of movie S4. The multilayer of intercalation processes occurred in a different manner from that in S4.

References:

(1) Suzuki, Y.; Sazaki, G.; Matsumoto, M.; Nagasawa, M.; Nakajima, K.; Tamura, K. *Cryst. Growth Des.* **2009**, *9*, 4289.

(2) Sazaki, G.; Matsui, T.; Tsukamoto, K.; Usami, N.; Ujihara, T.; Fujiwara, K.; Nakajima, K. *J. Cryst. Growth.* **2004**, *262*, 536.

(3) Van Driessche, A. E. S.; Sazaki, G.; Otálora, F.; González-Rico, F. M.; Dold, P.; Tsukamoto, K.; Nakajima, K. *Cryst. Growth Des.* **2007**, *7*, 1980.

(4) Wen, R.; Lahiri, A.; Azhagurajan, M.; Kobayashi, S.-i.; Itaya, K. *J. Am. Chem. Soc.* **2010**, *132*, 13657.

(5) Coraux, J.; N'Diaye, A. T.; Busse, C.; Michely, T. *Nano Lett.* **2008**, *8*, 565.